AIP | Journal of Applied Physics

Analysis on switching mechanism of graphene oxide resistive memory device

Seul Ki Hong, Ji Eun Kim, Sang Ouk Kim, and Byung Jin Cho

Citation: J. Appl. Phys. **110**, 044506 (2011); doi: 10.1063/1.3624947
View online: http://dx.doi.org/10.1063/1.3624947
View Table of Contents: http://jap.aip.org/resource/1/JAPIAU/v110/i4
Published by the American Institute of Physics.

Analysis on switching mechanism of graphene oxide resistive memory device

Seul Ki Hong,[1] Ji Eun Kim,[2] Sang Ouk Kim,[2] and Byung Jin Cho[1,a)]
[1]*Department of Electrical Engineering, KAIST, 335 Gwahak-ro, Yuseong-gu, Daejeon 305-701, Korea*
[2]*Department of Materials Science and Engineering, KAIST, 335 Gwahak-ro, Yuseong-gu, Daejeon 305-701, Korea*

(Received 29 March 2011; accepted 14 July 2011; published online 22 August 2011)

Recently, a flexible resistive switching memory device using graphene oxide was successfully demonstrated. In this work, the new findings on the switching mechanism of the graphene oxide memory are presented through a comprehensive study on the switching phenomena. It has been found that the switching operation of graphene oxide resistive switching memory (RRAM) is governed by dual mechanism of oxygen migration and Al diffusion. However, the Al diffusion into the graphene oxide is the main factor to determine the switching endurance property which limits the long term lifetime of the device. The electrode dependence on graphene oxide RRAM operation has been analyzed as well and is attributed to the difference in surface roughness of graphene oxide for the different bottom electrodes. © *2011 American Institute of Physics*. [doi:10.1063/1.3624947]

I. INTRODUCTION

Resistive switching memory (RRAM) has been widely investigated because of its potential for high speed, low operation voltage and high packing density.[1] Most of RRAM devices reported up to date use metal oxides as the insulator layer, and have shown good electrical performance.[2,3] On the other hand, organic materials are also being investigated as the insulator layer for RRAM, specifically targeting for the flexible electronics application, where the metal oxides cannot be used.[4,5] Recently, graphene and related materials have won attention in various research fields due to their excellent electrical and mechanical properties. One of the interesting and promising applications of graphene is the flexible RRAM device using graphene oxide.[6,7] The graphene oxide based RRAM device has shown on/off current ratio of $\sim 10^3$, excellent retention performance, and excellent flexibility without degradation of memory performance upon bending down to 4 mm radius.[6] However, its switching mechanisms including electrode dependence of the switching property and the limiting factor for switching endurance are still not fully understood.

In this paper, systematic study on switching mechanism of graphene oxide RRAM is reported, including electrical, chemical, and physical analyses and an investigation of the structural dependence. The results are expected to provide scientific basis for the design of graphene oxide based memory devices.

II. EXPERIMENTS

Graphene oxide was prepared by modified Hummer's method from graphite.[8] Graphene oxide solution is comprised of graphene oxide flakes, H_2O and methanol. The resistive switching memory has a metal-insulator-metal (MIM) capacitor structure, where graphene oxide was used as the insulator layer. Bottom electrode, such as ITO, Pt, or Al was deposited on glass or SiO_2 substrates and exposed to UV light to improve the adhesion of graphene oxide to the bottom electrode. The graphene oxide layer on bottom electrode was deposited by spincoating with N_2 blowing.[9] The N_2 blown on the electrode surface can improve the uniformity of graphene oxide layer and remove the solvent in graphene oxide solution. The samples were then annealed for 1h at 100 °C. XPS analysis was conducted using 500 μm circle pattern of Al/graphene oxide/ITO structure where the graphene oxide thickness was 30 nm. The beam spot for XPS analysis was within 100×100 μm^2. For cell area dependence experiment, MIM structures with different diameters of 180 μm, 200 μm, 300 μm, and 500 μm were used. For analysis of the graphene oxide surface, 5×5 μm area was scanned by AFM(PSIA) after an annealing process.

III. RESULTS AND DISCUSSION

The switching and endurance properties of graphene oxide RRAM comprised of Al/GO (30 nm thickness)/ITO are shown in Fig. 1. The device shows a typical bipolar resistive switching (BRS) property. The stable resistive switching between a high resistance state (HRS) and low resistance state (LRS) is clearly observed, with on/off current ratio of $\sim 10^3$ and set/reset voltages of within ± 2 V. The on/off current ratio remains stable as long as the device shows switching behavior, as shown in Fig. 1(b). Such a good switching behavior was also well demonstrated on flexible substrate in a previous work by the authors.[6] After approximately 100 times of repeated switching, however, the device failed to show switching, thus indicating the end of lifetime as a switching device. However the failure mechanism must be different from that of the conventional oxide based RRAM because the resistance value after failure settles

a)Author to whom correspondence should be addressed. Electronic mail: bjcho@ee.kaist.ac.kr.

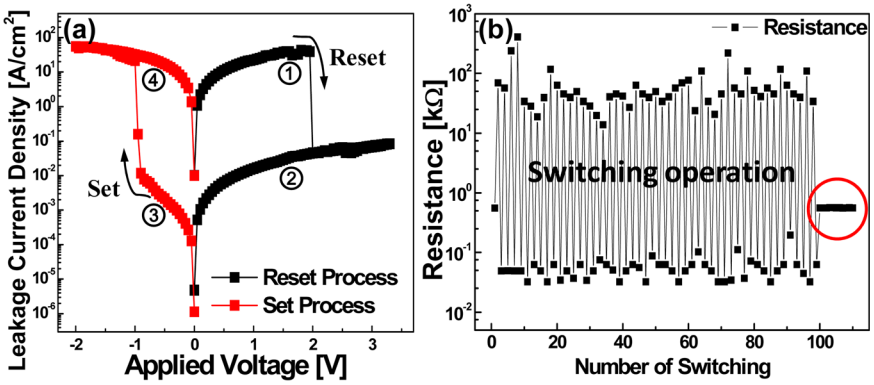

FIG. 1. (Color online) (a) The electrical switching and (b) endurance properties of graphene oxide RRAM consisted of Al/GO(30 nm thickness)/ITO structure.

somewhere in the middle of HRS and LRS, whereas the failure of the conventional RRAM caused by oxide breakdown always shows LRS value after breakdown. Therefore, understanding on this switching failure mechanism is very important to improve the endurance performance of the graphene oxide RRAM.

As the first step to identify the switching mechanism, an analysis of the current (I) – voltage (V) relationship of the memory device was performed. Figure 2 shows the I–V curves of the device in a double logarithmic scale under four different situations of memory operation. In RRAM operation, it has already well been characterized that ohmic contact relationship is described by $I(V)=\alpha V$ while space charge limited current (SCLC) is given by $I(V)=\alpha V+\beta V^2$ (Refs. 10 and 11). The indicated numbers in the figure denote the slope values of the *log I – log V* curve. It should be noted that the slopes of the curves are mostly ~ 1 except for the case of negative HRS immediately before the occurrence of the set operation, which is roughly two. The slope value of at two indicates that the switching from HRS to LRS is controlled by SCLC which is known to be triggered by oxygen deficiency in the dielectric layer. Oxygen vacancies and electron traps are easily generated in graphene oxide layer, and they can construct electron hopping path which changes the resistance state.[12]

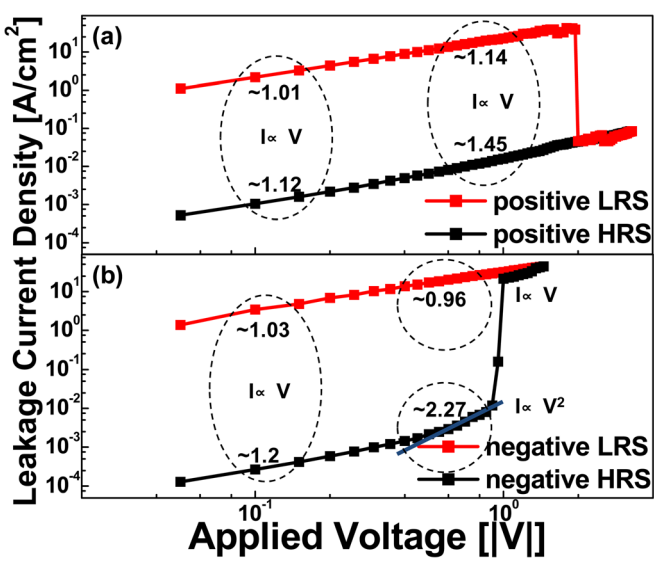

FIG. 2. (Color online) The current (I) – voltage (V) curves of the device in a double logarithmic scale under four different situations of the memory operation. The indicated numbers mean the slope value of *log I – log V* curve.

In order to obtain more direct confirmation of the oxygen controlled switching mechanism, oxygen depth profile in graphene oxide layer was analyzed by XPS and the results are shown in Fig. 3. The circled numbers in the drawing at the right upper corner of the figure indicate the analysis points within the graphene oxide layers in each state and the corresponding data for each number are shown in the O1s spectrum data plot. The O1s spectrum is divided into two major peaks reflecting C-OH and C=O bonding. The inset tables show relative quantities when the C=O bonding in the nearest top electrode is taken as a reference. In HRS, C-OH bonding peak decreases with depth, while in LSR, C=O bonding peak increases with depth. The distribution of the oxygen functional group density is remarkably changed with the resistance states, clearly indicating oxygen migration by electrical field within the graphene oxide layer. Therefore, it is reasonable to conclude that the oxygen migration is the main mechanism for switching operation in graphene oxide RRAM. However, this data alone cannot provide information on what determines the device endurance property, that is, its switching lifetime.

In order to ascertain whether any chemical composition change occurs in the graphene oxide upon repeated switching; a further XPS analysis was performed at the early stage of the switching as well as the later stage. Here, the 'early stage' means after two times of switching only and the 'later stage' means after more than 50 times of switching, as illustrated in the inset of Fig. 4. A total of five samples were prepared; each samples of LRS and HRS for the early stage and later stage, respectively, and one sample for the failure state. From the XPS results in Fig. 4, the HRS and LRS show different oxygen profiles near the top electrode. In LRS, oxygen percentage drops near the top electrode, indicating the generation of oxygen deficient region. This confirms again the oxygen-driven switching mechanism. However, there is not a distinct difference in oxygen profiles between not a distinct the early and later stages for the same resistance states. This suggests that oxygen movement is not the main factor which determines the device endurance property, i.e., the device lifetime. Another possible mechanism is the effect of

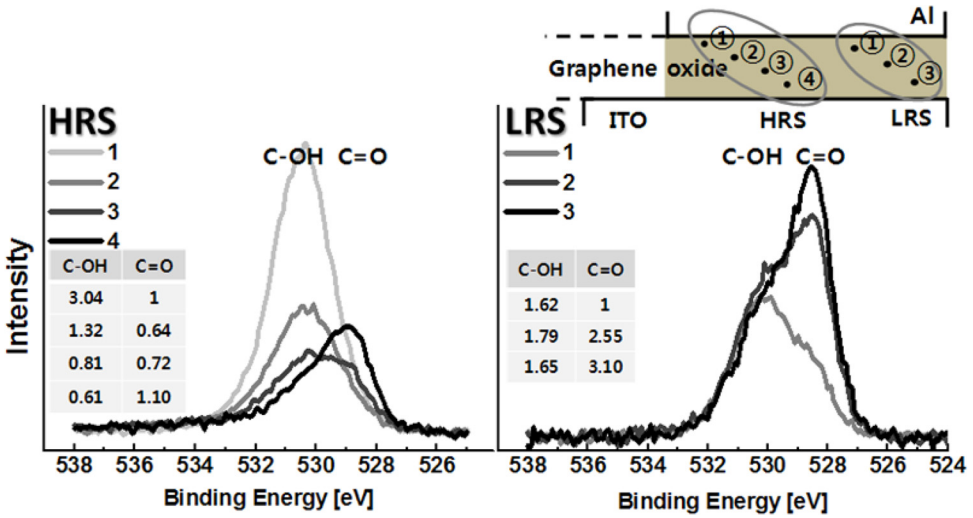

FIG. 3. (Color online) The oxygen depth profile in graphene oxide layer by XPS analysis. The circled numbers in the drawing at the right upper corner indicates the analysis points in each state and the corresponding data for each number are shown in the O1s spectrum data plot.

electrode, as some of RRAM devices have switching mechanism based on diffusion of electrode materials into the dielectrics.[13,14] Since our samples use aluminum electrode, Al depth profiles were analyzed for the same five samples mentioned in Fig. 4. XPS analysis points are illustrated in Fig. 5(a). In LRS, Al is detected between top and bottom electrodes as shown in Fig. 5(b) and 5(c). In addition, the Al peaks for the early stage and later stage are not substantially different. This indicates that the formation of Al conducting filament also accounts for the switching operation, and the Al diffusion does not decrease with the repeating switching cycle. On the other hand, in HRS, Al-O peaks are detected in the early stage of switching but no Al peaks are detected as shown in Fig. 5(d). After a number of switching cycles, however, a significant number of Al peaks are detected near the Al electrode [Fig. 5(e)], although the resistivity of the graphene oxide is still high. It should be noted that at the positions of ③, ④ which are far from the Al electrode, the Al peaks are still not detected as can be seen in Fig. 5(e). Once the device goes into the failure state, the Al-O peaks show no variation with graphene oxide depth; however the Al peaks are detected throughout the graphene oxide depth, indicating the formation of the Al conducting filament. This result clearly indicates that the long term reliability of the graphene oxide memory is governed by Al diffusion into the graphene oxide layer, and the switching operation itself is

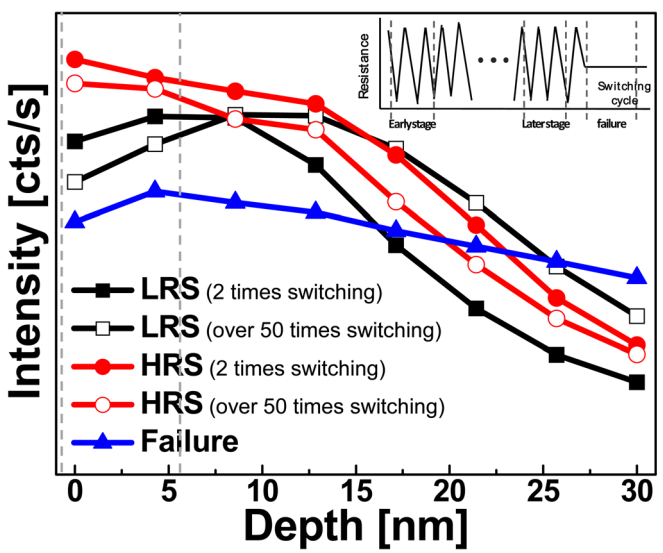

FIG. 4. (Color online) The depth XPS analysis about oxygen concentration. Total five samples were prepared; each samples of LRS and HRS for early stage and later stage, and one sample for failure state. 'Early stage' means after two times of switching only and 'later stage' means after over 50 times of switching as indicated in the inset drawing.

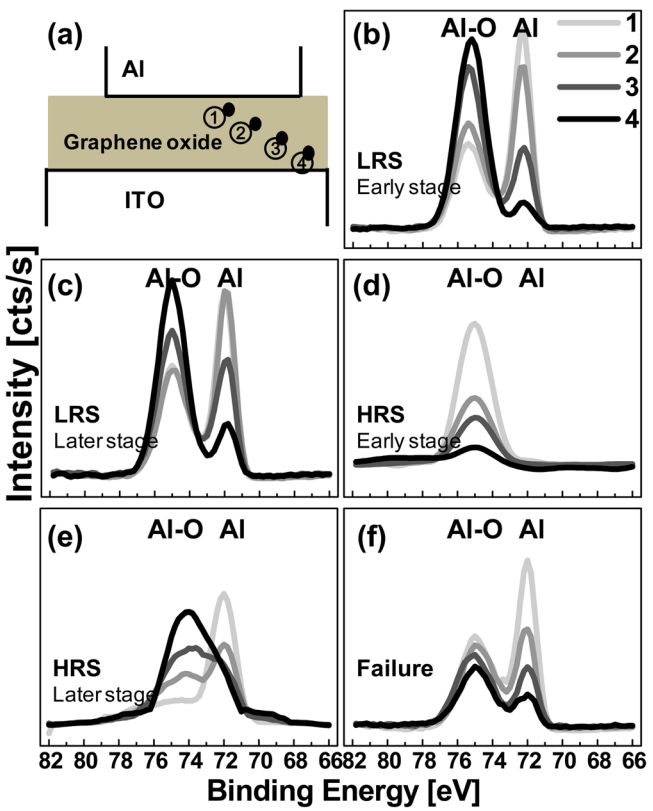

FIG. 5. (Color online) The Al depth profiles were analyzed for the same five samples used in Fig. 4. (a) XPS analysis points; (b) LRS for early stage; (c) LRS for later stage; (d) HRS for early stage; (e) HRS for later stage; (f) failure state.

controlled by dual mechanism of oxygen migration and Al diffusion.

As it has been found that the switching of the graphene oxide occurs by dual mechanism of oxygen migration and Al diffusion, a further analysis was performed to identify which factor is more dominant in switching operation. If the conducting filament formation by Al diffusion is the major factor of switching operation, leakage current in LRS should have no dependence on cell size as the conducting filament is a local phenomenon. If the switching is mainly governed by the migration of oxygen, leakage current must be proportional with cell size.[15] For this analysis, four different areas of circular patterns with 180 μm, 200 μm, 300 μm, and 500 μm diameters were fabricated and measured. The results in Fig. 6 show that the leakage current has a linear relationship with cell size. Therefore, it can be concluded that even though the switching has dual mechanism, the dominant mechanism of the switching of graphene oxide memory is the 'oxygen migration.'

While the major mechanism of switching operation has been clarified, another aspect should be elucidated—the dependence of the electrode. This is necessary because, according to our experiments, the switching operation of graphene oxide memory is observed only under some specific combinations of electrode materials. We tested a number of combinations of electrode materials and the results are summarized in Table I. Here, 'breakdown' means that device cannot return to HRS (off-state) once the device goes into the LRS. Among many combinations we tested, only two combinations (Al/ITO and Al/Pt) show stable and good switching operation performance. The Al/Al combination has the switching operation, but it is not stable and shows large sample-to-sample variation and easily changes to breakdown state. Many other combinations show breakdown once the voltage is applied, while some others show neither breakdown nor switching operation. In our experiment, the Au/GO/Pt structure does not show a resistive switching operation whereas a successful switching operation using the same structure has been reported in other literature.[16] This discrepancy shows that different fabrication processes can also affect the switching operation, because the two groups have used quite different fabrication processes, especially regarding the deposition step of GO and the thermal budget.

It also should be noted that not all the devices with aluminum top electrode in the present study show switching operation. Therefore, we also examined the effect of the bottom electrode. The contact angles of graphene oxide solution on four different surfaces of ITO, TaN, Au, and Pt were examined. For each electrode material, the effect of UV

TABLE I. Dependence of electrode materials on switching operation. Here, breakdown means that device cannot return to HRS once the device goes in to the LRS. Many combinations show breakdown once the voltage is applied, while some other show neither breakdown nor switching operation. Only three combinations in our experiment (Al/ITO, Al/Pt, and Al/Al) showed switching operation.

Top	Bottom	Switching	Breakdown
Al	ITO	O	X
Al	Pt	O	X
Al	Al	Δ	O
Al	Pd	X	O
Al	TaN	X	O
Au	Al	X	O
TiN	Al	X	O
Au	Pt	X	O
Au	ITO	X	O
Cr	Al	X	X
Cr	ITO	X	X
Cr	TaN	X	X
Cr	Pt	X	X
TiN	ITO	X	X
TiN	Pt	X	X
TiN	TaN	X	X
Au	Pd	X	X

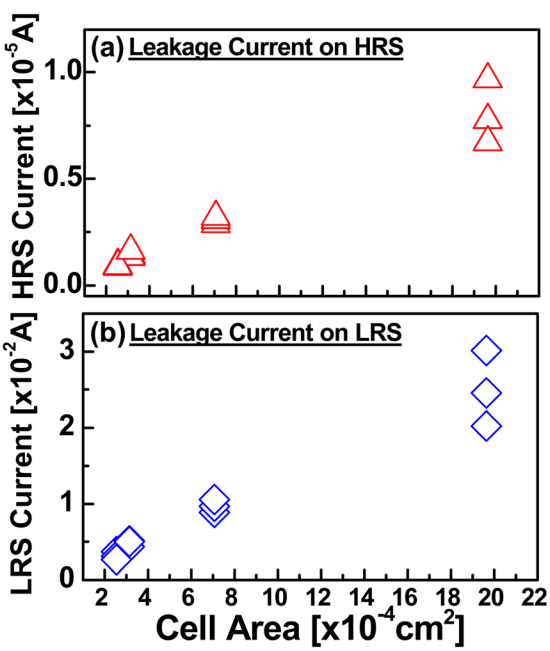

FIG. 6. (Color online) Cell area dependence of leakage current in (a) HRS and (b) LRS. The leakage current has a linear relationship with cell size, indicating that the leakage is not due to a local phenomenon.

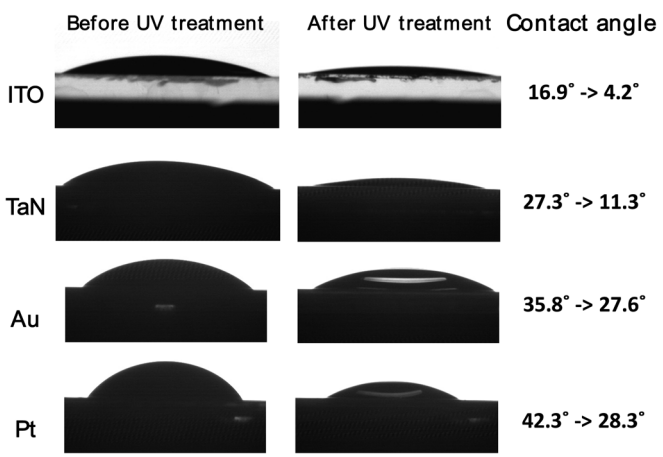

FIG. 7. The contact angles of graphene oxide solution on four different surfaces of ITO, TaN, Su, and Pt. UV treatment is done to promote adhesion.

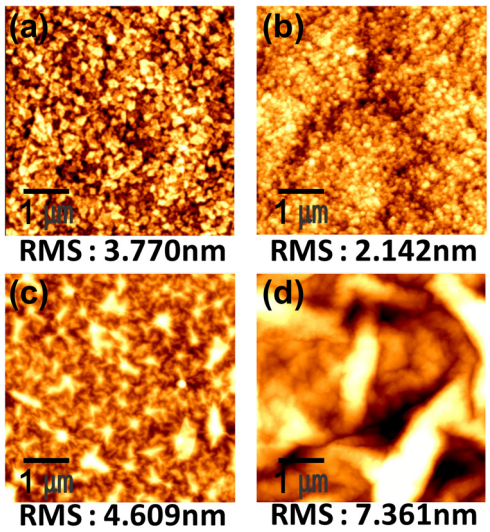

FIG. 8. (Color online) The surface roughness of graphene oxide after deposition on various bottom electrodes; (a) ITO, (b) Pt, (c) Al and (d) Au. The measurement was done by AFM.

treatment, which is carried out promote adhesion of graphene oxide to the bottom electrode, was tested as well. The contact angle measurement results are shown in Fig. 7. The results show no clear correlation between switching operation and contact angle. ITO and Pt show good switching performance but one shows lowest while the other shows highest contact angle. Therefore, we must rule out the contact angle and adhesion of graphene oxide on the bottom electrode as the reason for the electrode dependence.

The surface roughness of graphene oxide after deposition on the bottom electrode was next examined. According to the fabrication procedure of the device, the graphene oxide was annealed at 100 °C for 1 h after deposition on four different electrode surfaces (ITO, Pt, Au and Al), and the surface roughness was monitored by AFM and SEM. Surprisingly, the graphene oxide surface was very different for the different electrodes, as can be seen in Fig. 8. The graphene oxide on the ITO and Pt substrates respectively shows low roughness values of 3.77 nm and 2.14 nm. For the case of Al, the roughness displayed a wide deviation among different locations on the sample. In other cases, such as TaN and Au, the graphene oxide surface has a lot of cracks and the rms roughness is also quite large. If the graphene oxide has such cracks and rough surface, electrode material may easily penetrate and then construct conducting filament which hinders the switching operation. This difference among different electrodes is likely caused by the different thermal properties of the electrodes and graphene oxide, as the roughness measurement was performed after annealing and the annealing is required for the device fabrication. The surface roughness tendency of graphene oxide after annealing is consistent with the dependence of the switching operation on the electrode material, as shown in Table I. Therefore, it is speculated that the interaction between graphene oxide and bottom electrode is the main factor for dependence of the switching property on the electrode.

V. CONCLUSIONS

Through a detailed analysis of the switching mechanism of graphene oxide RRAM, it has been found that the resistive switching occurs by dual mechanism of oxygen migration and Al diffusion, and the oxygen migration is dominant factor. However, the long term reliability is governed by Al diffusion and the lifetime of the device is limited by the permanent formation of Al conducting filament. The dependence of the switching operation on the electrode has also been clarified. Such new findings presented in this work will be important for understanding on the memory operation principle of graphene oxide RRAM and provide the clues for further improvement of the device performance.

ACKNOWLEDGMENTS

This work was supported by the National Research Foundation of Korea (NRF) Research Grant Nos. 2008-2002744 and 2010-0029132.

[1]R. Waser and M. Aono, Nature Mater. **6**, 833 (2007).
[2]D. H. Kwon, K. M. Kim, J. H. Jang, J. M. Jeon, M. H. Lee, G. H. Kim, X. S. Li, G. S. Park, B. R. Lee, S. W. Han, M. Y. Kim, and C. S. Hwang, Nat. Nanotechnol. **5**, 148 (2009).
[3]T. Mikolajich, M. Salinga, M. Kund, and T. Kever, Adv. Eng. Mater. **11**, 235 (2009).
[4]M. Colle, M. Buchel, and D. M. de Leeuw, Org. Electron. **7**, 305 (2006).
[5]F. Verbakel, S. C. J. Meskers, and R. A. J. Janssen, Appl. Phys. Lett. **91**, 192103 (2007).
[6]S. K. Hong, J. E. Kim, S. O. Kim, S-Y. Choi, and B. J. Cho, IEEE Electron Device Lett. **31**, 1005 (2010).
[7]H. Y. Jeong, J. Y. Kim, J. W. Kim, J. O. Hwang, J-E. Kim, J. Y. Lee, T. H. Yoon, B. J. Cho, S. O. Kim, R. S. Ruoff, and S-Y. Choi, Nano Lett. **10**, 4381 (2010).
[8]W. S. Hummers and R. E. Offeman, J. Am. Chem. Soc. **80**, 1339 (1958).
[9]J. T. Robinson, M. Zalalutdinov, J. W. Baldwin, E. S. Snow, Z. Q. Wei, P. Sheehan, and B. H. Houston, Nano Lett. **8**, 3441 (2008).
[10]R. A. Miller, Nature **182**, 1296 (1958).
[11]T. Harada, I. Ohkubo, K. Tsubouchi, H. Kumigashira, T. Ohnishi, M. Lippmaa, Y. Matsumoto, H. Koinuma, and M. Oshima, Appl. Phys. Lett. **92**, 222113 (2008).
[12]D. Joung, A. Chunder, L. Zhai, and S. I. Khondaker, Appl. Phys Lett. **97**, 093105 (2010).
[13]J. B. Park, M. S. Jo, J. M. Lee, S. J. Jung, S. H. Kim, W. T. Lee, J. H. Shin, and H. S. Hwang, IEEE Electron Device Lett. **32**, 63 (2011).
[14]D.-H. Kwon, K. M. Kim, J. H. Jang, J. M. Jeon, M. H. Lee, G. H. Kim, X.-S. Li, G.-S. Park, B. R. Lee, S. W. Han, M. Y. Kim, and C. S. Hwang, Nat. Nanotechnol. **5**, 148 (2010).
[15]R. Waser, R. Dittmann, G. Staikov, and K. Szot, Adv. Mater. **21**, 2632 (2009).
[16]C. L. He, F. Zhuge, X. F. Zhou, M. Li, G. C. Zhou, Y. W. Liu, J. Z. Wang, B. Chen, W. J. Su, Z. P. Liu, Y. H. Wu, P. Cui, and R.-W. Li, Appl. Phys. Lett, **95**, 232101 (2009).